

# Intrinsic bounds of a two-qudit random evolution

A. Z. Khoury<sup>1</sup>, A. M. Souza<sup>2</sup>, L. E. Oxman<sup>1</sup>, I. Roditi<sup>2</sup>, R. S. Sarthour<sup>2</sup>, I. S. Oliveira<sup>2</sup>

1- Instituto de Física, Universidade Federal Fluminense, 24210-346, Niterói - RJ, Brazil.

2- Centro Brasileiro de Pesquisas Físicas, Rua Dr. Xavier Sigaud 150, 22290-180, Rio de Janeiro - RJ, Brazil.

We investigate entangled qudits evolving under random, local  $SU(d)$  operations and demonstrate that this evolution is constrained by intrinsic bounds, showing robust features of two-qudit entangled states that can be useful for fault tolerant implementations of phase gates. Our analytical results are supported by numerical simulations and confirmed by experiments on liquid-state nuclear magnetic resonance qubits.

PACS numbers: 03.67.Mn, 03.65.Vf, 03.67.Pp

The development of quantum technologies is challenged by the unavoidable action of the environment and uncontrollable experimental imperfections. These effects cause errors in quantum algorithms and limit the scalability of quantum devices. Strategies to isolate the physical systems used for quantum information tasks and to identify some of their features immune to those undesired effects are in course. The use of engineered reservoirs [1–3], decoherence free subspaces [4], geometrical phases [5], topologically protected systems [6] and dynamical decoupling (see for example [7–10]) have been considered as potential means for robust quantum computation. The role of entanglement in the geometric phase acquired by entangled quantum systems has motivated a great deal of interesting research works [11, 12]. In particular, it has been theoretically predicted [13, 14] and experimentally demonstrated [15, 16] that the geometric phase acquired by maximally entangled qubits is discrete, restricted to integer multiples of  $\pi$ . Later, fractional phases were predicted for maximally entangled systems with arbitrary dimension  $d$  (*qudits*) [17–20] and for multiple qubits [21, 22]. Quantum algorithms employing qudits have also been considered in the literature [23–25].

In this work we demonstrate an intriguing feature of entanglement regarding the evolution of a two-qudit state under arbitrary local  $SU(d)$  transformations. The inner product (overlap) between the transformed and the initial states is shown to be confined within a nontrivial boundary in the complex plane. This boundary is deduced analytically, confirmed by numerical simulations with random local  $SU(d)$  transformations and, furthermore, experimentally verified with nuclear magnetic resonance.

Let us consider a two-qudit quantum state evolution

$$|\psi(t)\rangle = \sum_{i,j=1}^d M_{ij}(t)|ij\rangle, \quad (1)$$

where  $M$  is the coefficient matrix of the quantum state expansion in the computational basis  $\{|ij\rangle\}$ . It will be useful for our purposes, to write the coefficient matrix in its polar decomposition:

$$M(t) = e^{i\theta(t)} Q(t) S(t), \quad (2)$$

where three sectors can be identified:

- The  $U(1)$  sector represented by the overall phase factor  $e^{i\theta(t)}$ .
- The  $SU(d)$  sector given by  $S(t) \in SU(d)$ .
- The Hermitian sector  $Q(t) = Q^\dagger(t)$ .

Under local unitary transformations, each sector follows an independent time evolution. Indeed, let  $U_A(t) = e^{i\theta_A(t)}\bar{U}_A(t)$  and  $U_B(t) = e^{i\theta_B(t)}\bar{U}_B(t)$  be the local unitary transformations applied to qudits  $A$  and  $B$ , with  $\bar{U}_A(t)$  and  $\bar{U}_B(t) \in SU(d)$ . In this case the evolution in each sector is given by

$$\begin{aligned} \theta(t) &= \theta(0) + \theta_A(t) + \theta_B(t), \\ Q(t) &= \bar{U}_A(t) Q(0) \bar{U}_A^\dagger, \\ S(t) &= \bar{U}_A(t) S(0) \bar{U}_B^T. \end{aligned} \quad (3)$$

It will be convenient to adopt the basis leading to the Schmidt decomposition of the initial state, so that  $M_{ij}(0) = M_{jj}(0) \delta_{ij}$  and  $M_{jj}(0) \in \mathbb{R}$ . In this case,  $\theta(0) = 0$  and  $S(0) = \mathbb{1}$ . Moreover, we shall assume that the two qudits are locally operated with  $SU(d)$  transformations ( $\theta_A = \theta_B = 0$ ), making the  $U(1)$  sector stationary. Note that local  $SU(d)$  transformations are naturally realized in spin systems interacting with an external magnetic field, since the energies of the spin eigenstates are symmetrically shifted in this case. As we will see, this makes nuclear magnetic resonance (NMR) the ideal platform for the experimental investigation.

The intrinsic bounds imposed on entangled qudits are more pronounced for maximally entangled states, as we will see shortly. In this case,  $Q(0) = \mathbb{1}/\sqrt{d}$  and the Hermitian sector remains stationary for arbitrary local transformations. Then, the two-qudit state evolution will be restricted to the  $SU(d)$  sector of the coefficient matrix and the time dependent overlap between the evolved and the initial states will be

$$O(t) = \langle \psi(0) | \psi(t) \rangle = \text{Tr} [M^\dagger(0) M(t)] = \frac{\text{Tr} [S(t)]}{d}. \quad (4)$$

We now demonstrate that this overlap remains restricted to a confined area of the complex plane, whose perimeter depends on the dimension of the qudits. Since  $S(t) \in$

$SU(d)$  ( $\det S(t) = 1$ ), its eigenvalues are phase factors  $\{e^{i\phi_j(t)}\}$  ( $j = 1 \dots d$ ), constrained by the condition

$$F(\{\phi_j\}) = \sum_{j=1}^d \phi_j = 0. \quad (5)$$

In terms of these phase factors, the time dependent overlap is given by

$$O(t) = \frac{1}{d} \sum_{j=1}^d e^{i\phi_j(t)} = R e^{i\Phi}, \quad (6)$$

where  $R$  is the overlap absolute value and  $\Phi$  its phase. In order to find the contour of the overlap boundary in the complex plane, we need to determine  $R_{max}(\Phi)$ , the extrema of  $R$  for each phase  $\Phi$ . For a given eigenvalue configuration  $\{\phi_j\}$ , the overlap absolute value can be deduced from the real part of Eq. (6) as

$$R(\{\phi_j\}) = \frac{1}{d} \sum_{j=1}^d \cos(\phi_j - \Phi). \quad (7)$$

At the same time, a second constraint can be immediately derived from the imaginary part

$$G(\{\phi_j\}) = \frac{1}{d} \sum_{j=1}^d \sin(\phi_j - \Phi) = 0. \quad (8)$$

We are now able to find  $R_{max}(\Phi)$  under these two constraints using Lagrange multipliers. For this end, we define

$$L(\{\phi_j\}, \lambda_f, \lambda_g) = R(\{\phi_j\}) + \lambda_f F(\{\phi_j\}) + \lambda_g G(\{\phi_j\}), \quad (9)$$

where  $\lambda_f$  and  $\lambda_g$  are Lagrange multipliers. The constrained extrema of  $R$  are obtained from the solutions of

$$\frac{\partial L}{\partial \phi_k} = \frac{-\sin(\phi_k - \Phi) + \lambda_g \cos(\phi_k - \Phi)}{d} + \lambda_f = 0,$$

from which we readily derive the condition

$$\frac{1}{d} \sin(\Phi + \theta - \phi_k) = \Lambda, \quad (10)$$

where the Lagrange multipliers were replaced by the more convenient variables  $\theta = \arctan \lambda_g$  and  $\Lambda = -\lambda_f \cos \theta$ . These variables, as well as condition (10), can be easily interpreted in terms of a geometric construction on the complex plane, as shown in Fig.(1). Consider the numbers  $e^{i\phi_k}/d$  ( $1 \leq k \leq d$ ) rotating in the complex plane constrained by conditions (5) and (8). The overlap is maximized when  $d-1$  among these numbers turn around the complex plane with the same phase  $\phi(t)$  and the remaining one turns in the opposite sense with phase  $(1-d)\phi(t)$ . Of course, there is an intrinsic permutation

symmetry with respect to which one of the eigenvalues will follow the opposite evolution, so we may choose the solution  $\phi_k = \phi \forall k \in [1, d-1]$ , while  $\phi_d = (1-d)\phi$ . This permutation symmetry is broken in the case of non maximal entanglement. The geometric interpretation of  $\theta$  and  $\Lambda$  becomes clear when we represent the line connecting the numbers  $e^{i\phi_k}/d$ , as depicted in Fig. (1) for the  $SU(3)$  case. The distance between this connecting line and the origin of the complex plane is  $\Lambda$ , while  $\theta$  is the angle between this line and the graphic representation of the overlap  $O(t)$ .

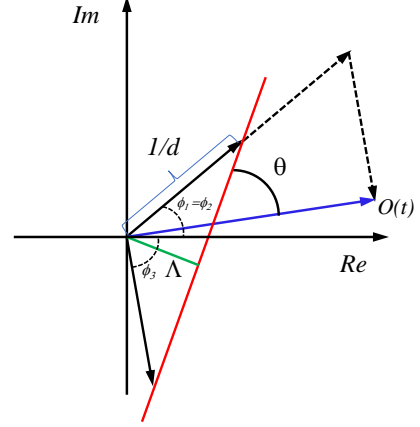


FIG. 1: Graphic representation of the  $SU(3)$  eigenvalues and the maximum state overlap, showing the geometric meaning of the Lagrange variables.

It will be easier to express our analytical results in parametrized form as functions of  $\phi$ . From the geometric construction of Fig. (1), the following expressions can be deduced

$$\begin{aligned} R_{max} &= \sqrt{1 - 4 \left( \frac{d-1}{d^2} \right) \sin^2 \left( \frac{d\phi}{2} \right)}, \\ \Phi &= \phi + \arg(d-1 + e^{-id\phi}), \\ \theta &= \frac{\pi}{2} - \Phi - \frac{d-2}{2} \phi, \\ \Lambda &= \frac{1}{d} \cos \left( \frac{d\phi}{2} \right). \end{aligned} \quad (11)$$

Note that the maximum overlap reaches unity when  $\phi = 2n\pi/d$ , the allowed topological phases for two-qudit systems evolving under local  $SU(d)$  operations. The minimum value of  $R_{max}$  is  $1 - 2/d$  for  $\phi = (2n+1)\pi/d$ . By varying  $\phi$  in the interval  $[0, 2\pi]$ , we can draw the polar plot of the overlap boundary in the complex plane. This boundary defines a closed curve with exactly  $d$  branches covered by the intervals  $\phi \in [2n\pi/d, 2(n+1)\pi/d]$  ( $0 \leq n \leq d-1$ ). For maximally entangled qubits, the overlap boundary collapses to a line segment on the real axis defined by the interval  $[-1, 1]$ .

In order to illustrate the overlap boundaries for different dimensions, we present in Fig. (2) the analyti-

cal contours given by Eqs. (11) (red line curves) and the numerical simulations with random  $SU(d) \times SU(d)$  transformations (blue line dots) for  $d = 2, 3$  and 4. The numerical results show clear confinement within the analytical boundary.

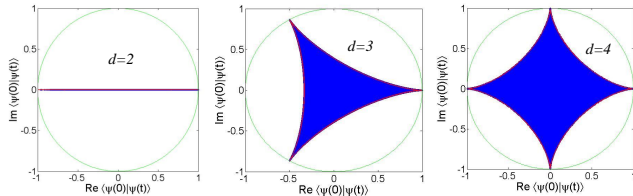


FIG. 2: Evolution of the two-qudit overlap under random local  $SU(d)$  operations for  $d = 2, 3$  and 4. The analytical boundary is displayed in red (online) and the results of numerical simulations are displayed in blue (online) dots. The unit circle is indicated in green (online) for reference.

Following the same geometric construction, the inclusion of partial entanglement is straightforward but lengthy and we shall leave the detailed description to a future contribution. As a universal behavior in any dimension, the sharp edges between the boundary branches are smoothed as entanglement diminishes until the boundary degenerates to the unit circle when product states are reached. For qubits, this results in inflation of the line segment on the real axis to an ovoid and finally to the unit circle. For a pair of qubits initially prepared in a pure state with concurrence  $C$ , the solution for the maximum overlap is

$$R_{max} = \sqrt{1 - C^2 \sin^2 \phi},$$

$$\Phi = \arctan\left(\sqrt{1 - C^2} \tan \phi\right). \quad (12)$$

For product states ( $C = 0$ ), one trivially obtains  $R_{max} = 1$  and  $\Phi = \phi$ , what corresponds to the unit circle boundary. For maximally entangled states ( $C = 1$ ), we have  $R_{max} = |\cos \phi| \in [0, 1]$  and  $\Phi$  becomes discrete, assuming only 0 or  $\pi$ , the two-qubit topological phases predicted by Milman and Mosseri [13, 14].

Experimental observations of geometrical phases are only achievable using interferometric approaches. Figure 3a illustrates the scheme of a simple interferometer. Photons entering the interferometer are split into two perpendicular paths labeled as  $|0\rangle$  and  $|1\rangle$ . On the path  $|1\rangle$  the photons undergo a phase shift due to the application of an unitary evolution  $U$ . After the paths are recombined using the beam splitter the probability for measuring the states  $|0\rangle$  or  $|1\rangle$  contains information about the phase shift between the paths.

In NMR, the analog of the interferometry model described above can be implemented using the eigenstates of an auxiliary spin-1/2 to emulate two photon paths [16, 26–28] (see figure 3b). At the beginning of the interferometry operation the system we want to probe is

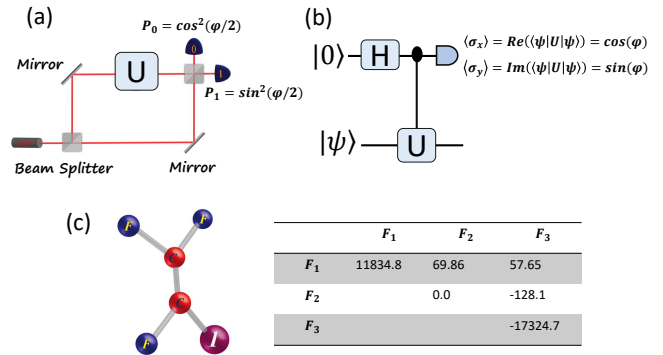


FIG. 3: (a) Scheme of an optical interferometer. The phase shift introduced by the unitary  $U$  can be determined measuring the probabilities,  $P_0$  and  $P_1$ . (b) The quantum circuit analog to the interferometer based on one auxiliary qubit. The phase shift on the system qubit is determined measuring the average value of the Pauli matrices,  $\sigma_x$  and  $\sigma_y$ , of the auxiliary qubit. (c) The structure and parameters of the NMR 3-qubit Iodotrifluoroethylene molecule. The diagonal terms in the table are the chemical shifts written in relation to the fluorine nucleus labeled as  $F_2$ . The off diagonal terms are the coupling constants, all parameters are shown in Hz.

prepared in a given two-qubit state  $|\psi\rangle$ , whereas the auxiliary spin is prepared in the superposition state  $(|0\rangle + |1\rangle)/\sqrt{2}$ , by applying a Hadamard gate on the state  $|0\rangle$ . The application of the controlled unitary operator  $U$  provides the state  $(|0\rangle|\psi(0)\rangle + |1\rangle|\psi(t)\rangle)/\sqrt{2}$ , where  $|\psi(t)\rangle = U|\psi(0)\rangle = e^{i\phi}|\psi(0)\rangle$ . When a measurement is performed on the auxiliary spin, its normalized  $x - y$  magnetization components on the plane, which are proportional to the average value of the Pauli matrices, are directly related to the overlap between the states.

To perform the experiment we have used an ensemble of identical and non-interacting molecules in liquid state at room temperature, where nuclear spins are employed as qubits. The quantum state of the ensemble is prepared, from the thermal equilibrium, in the so called pseudo-pure state (PPS) [32]:

$$\rho = (1 - \epsilon)\frac{I}{D} + \epsilon|\psi\rangle\langle\psi|. \quad (13)$$

Since the maximally mixed part  $I/D$  does not produce an observable signal, the overall NMR signal arises only from the pure state part  $|\psi\rangle\langle\psi|$  where the factor  $\epsilon \approx 10^{-5}$  is the thermal polarization and  $D$  is the dimension of the Hilbert space. Under a suitable normalization, the state (13) is equivalent to that from a system in a pure state  $|\psi\rangle$ , and therefore, can be used to test different features of pure entangled states [33–35].

The experiment was performed at room temperature, using a 500 MHz Varian NMR spectrometer and an ensemble of Iodotrifluoroethylene ( $C_2F_3I$ ) molecules dissolved in deuterated acetone. This molecule (see figure 3c) contains three spin-1/2  $^{19}F$  nuclei, where two fluorine nuclei are used to encode the state  $|\psi\rangle$  and one fluorine

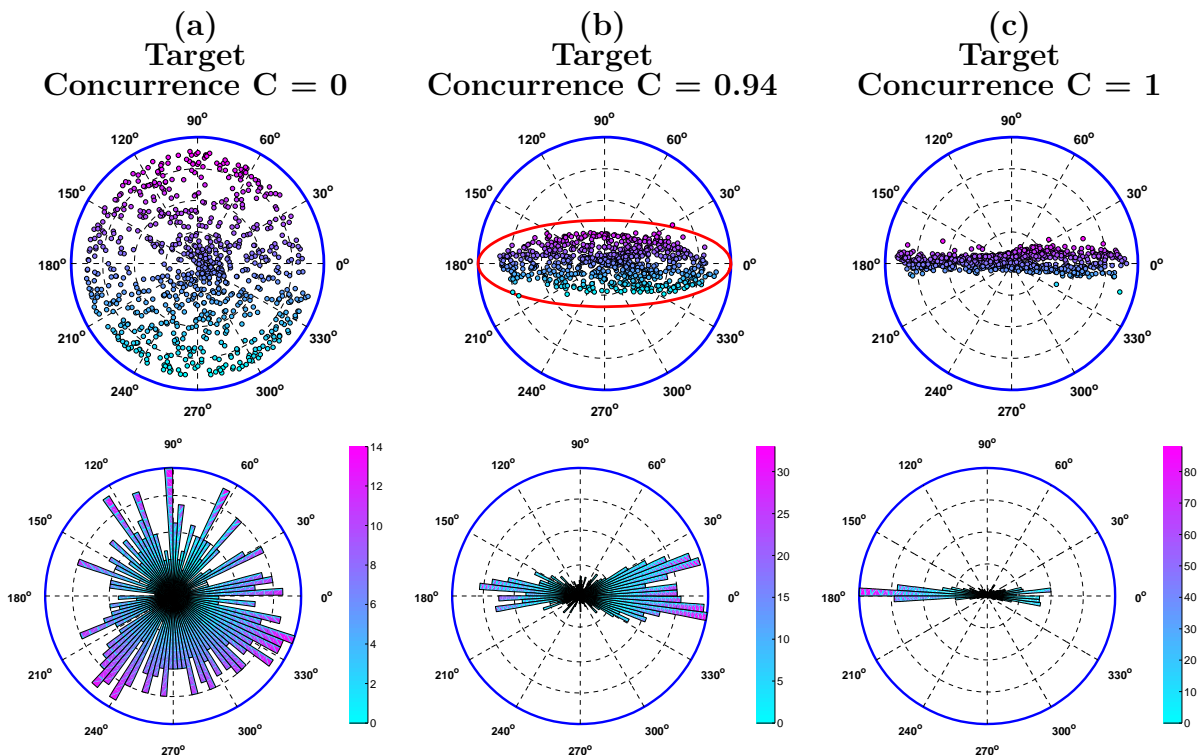


FIG. 4: Geometrical phase acquired under random unitary evolutions for three different states: (a) The separable state  $|00\rangle$ , (b) the partial entangled state  $\cos(7\pi/36)|00\rangle + \sin(7\pi/36)|11\rangle$  and (c) the maximally entangled state  $(|00\rangle + |11\rangle)/\sqrt{2}$ . The top panel shows the overlap  $\langle\psi(0)|\psi(t)\rangle$  in the complex plane and the bottom panel shows the distribution of the geometrical phases in polar histograms.

nucleus is used as the auxiliary spin. The PPS was created using the control transfer gates technique [36], the actual pulse sequence used can be found in [28]. To implement gate operations we exploit standard Isech shaped pulses interleaved with periods of free evolutions. For combining all operations into a single pulse sequence we have used the techniques described in [29–31].

Figure 4 shows the overlap  $\langle\psi(0)|\psi(t)\rangle$  in the complex plane under 800 random unitaries for three states with different degrees of entanglement. The unitaries were applied only on a single qubit of the entangled pair and have the form  $U = R_x(\theta)R_z(\beta)$ , where  $\theta$  and  $\beta$  were randomly chosen from 0 to  $4\pi$ . The results clearly shows the confinement by the bounds (12). As the degree of entanglement is increased the acquired geometrical phase become more robust, being only  $\pm\pi$  when the state is maximally entangled. The deviations from the theory are due to decoherence processes and experimental imperfections on the control gates.

In conclusion, we have investigated pairs of entangled qudits evolving under random, local  $SU(d)$  operations. More specifically we have analytically demonstrated that

the overlap between the  $SU(d)$  transformed and the initial state is confined within boundaries that only depend on the degree of entanglement. This feature was illustrated with numerical simulations and, moreover, experimentally verified with an NMR setup. Our results provide a step further in the direction of robust quantum computation and may find application for fault tolerant implementations of phase gates. They also open new perspectives for investigations of nontrivial bounds on multi-qubit systems, where fractional phases are expected as well [21, 22].

### Acknowledgments

Funding was provided by Coordenação de Aperfeiçoamento de Pessoal de Nível Superior (CAPES), Fundação de Amparo à Pesquisa do Estado do Rio de Janeiro (FAPERJ-BR), and Instituto Nacional de Ciência e Tecnologia de Informação Quântica (INCT-CNPq).

[1] N. A. Peters, J. B. Altepeter, D. A. Branning, E. R. Jeffrey, T.-C. Wei, P. G. Kwiat, Phys. Rev. Lett. **92**,

133601 (2004).

- [2] A. Aiello, G. Puentes, and J. P. Woerdman, *Phys. Rev. A* **76**, 032323 (2007).
- [3] M. Hor-Meyll, A. Auyuanet, C. V. S. Borges, A. Aragão, J. A. O. Huguenin, A. Z. Khoury, L. Davidovich, *Phys. Rev. A* **80**, 042327 (2009).
- [4] G. M. Palma, K. A. Suominen, A. K. Ekert, *Proc. R. Soc. London, Ser. A* **452**, 567 (1996).
- [5] J. A. Jones, V. Vedral, A. Ekert, and G. Castagnoli, *Nature (London)* **403**, 869 (2000).
- [6] A. Kitaev, *Ann. Phys. (N.Y.)* **303**, 2 (2003).
- [7] J. Zhang, A. M. Souza, F. D. Brandao and D. Suter *Phys. Rev. Lett.* **112**, 050502 (2014).
- [8] A. M. Souza, G. A. Alvarez, and D. Suter *Phys. Rev. Lett.* **106**, 240501 (2011).
- [9] A. M. Souza, G. A. Alvarez, and D. Suter *Phys. Rev. A* **86**, 050301(R) (2012).
- [10] A. M. Souza, R. S. Sarthour, I. S. Oliveira, and D. Suter *Phys. Rev. A* **96**, 062332 (2015).
- [11] E. Sjöqvist, *Phys. Rev. A* **62**, 022109 (2000).
- [12] B. Hessmo and E. Sjöqvist, *Phys. Rev. A* **62**, 062301 (2000).
- [13] P. Milman, and R. Mosseri, *Phys. Rev. Lett.* **90**, 230403 (2003).
- [14] P. Milman, *Phys. Rev. A* **73**, 062118 (2006).
- [15] C. E. R. Souza, J. A. O. Huguenin, P. Milman, and A. Z. Khoury, *Phys. Rev. Lett.* **99**, 160401 (2007).
- [16] J. Du, J. Zhu, M. Shi, X. Peng, D. Suter, *Phys. Rev. A* **76**, 042121 (2007).
- [17] L. E. Oxman and A. Z. Khoury, *Phys. Rev. Lett.* **106**, 240503 (2011).
- [18] A. Z. Khoury, L. E. Oxman, B. Marques, A. Matoso, and S. Pádua, *Phys. Rev. A* **87**, 042113 (2013).
- [19] A. Z. Khoury and L. E. Oxman, *Phys. Rev. A* **89**, 032106 (2014).
- [20] A. A. Matoso, X. Sánchez-Lozano, W. M. Pimenta, P. Machado, B. Marques, F. Sciarrino, L. E. Oxman, A. Z. Khoury, S. Pádua, *Phys. Rev. A* **94**, 052305 (2016).
- [21] M. Johansson, M. Ericsson, K. Singh, E. Sjöqvist, and M. S. Williamson, *Phys. Rev. A* **85**, 032112 (2012).
- [22] M. Johansson, A. Z. Khoury, K. Singh, and E. Sjöqvist, *Phys. Rev. A* **87**, 042112 (2013).
- [23] S. S. Bullock, D. P. OLeary, and G. K. Brennen, *Phys. Rev. Lett.* **94**, 230502 (2005).
- [24] A. Muthukrishnan, and C. R. Stroud, Jr., *Phys. Rev. A* **62**, 052309 (2000).
- [25] R. Ionicioiu, T. P. Spiller, and W. J. Munro, *Phys. Rev. A* **80**, 012312 (2009).
- [26] D. Suter, K. T. Mueller, and A. Pines, *Phys. Rev. Lett.* **60**, 1218 (1998).
- [27] A. Ghosh and A. Kumar, *Physics Letters A* **349**, 27-36 (2006).
- [28] F. Anvari Vind, A. Foerster, I. S. Oliveira, R. S. Sarthour, D. O. Soares-Pinto, A. M. Souza and I. Roditi, *Scientific Reports* **6**, 20789 (2016).
- [29] M. D. Bowdrey, J. A. Jones, E. Knill, and R. Laflamme, *Phys. Rev. A* **72**, 032315 (2005).
- [30] C. A. Ryan, C. Negrevergne, M. Laforest, E. Knill, and R. Laflamme, *Phys. Rev. A* **78**, 012328 (2008).
- [31] A. M. Souza, J. Zhang, C. A. Ryan, and R. Laflamme, *Nature Communications* **2169**, 1 (2011).
- [32] I.S.Oliveira, T.J. Bonagamba, R. S. Sarthour, J. C. C. Freitas and E. R. deAzevedo *NMR Quantum Information Processing (Amsterdam: Elsevier)* (2007).
- [33] A. M. Souza, A. Magalhes, J. Teles, E. R. deAzevedo, T. J. Bonagamba, I. S. Oliveira and R. S. Sarthour, *New J. Phys.* **10**, 033020 (2008).
- [34] Ren, Changliang; Lu, Dawei; Shi, Mingjun; et al., *Phys. Lett. A* **373**, 4222 (2009).
- [35] Richard J. Nelson, David G. Cory, and Seth Lloyd, *Phys. Rev. A* **61**, 022106 (2000).
- [36] M. Kawamura, B. Rowland and J. A. Jones *Phys. Rev. A* **82**, 032315 (2010).